Targeting prion-like protein doppel selectively suppresses tumor angiogenesis

Taslim A. Al-Hilal[1,2,3], Seung Woo Chung[1], Jeong Uk Choi[1], Farzana Alam[4], Jooho Park[1], Seong Who Kim[5], Sang Yoon Kim[2,6], Fakhrul Ahsan[3], In-San Kim[2,7], Youngro Byun[1,4]

Contents

Supplemental Experimental Procedures

Materials. Low molecular weight heparin (LMWH) with an average molecular weight of 4500 Da was obtained from Nanjing King-Friend Biochemical Pharmaceutical Company Ltd. (Nanjing, China). Cy5.5 NHS ester was purchased from Lumiprobe (Hallandale beach, FL). Deoxycholic acid (DOCA), *N*-ethyl-*N*-(3-dimethylaminopropyl) carbodiimide hydrochloride (EDAC), *N*-hydroxysuccinimide (NHS), 1,2-ethylenediamine (EDA), sodium cyanoborohydride, Hoechst 33258, protease inhibitor cocktail tablets (S8820), and phosphatase inhibitor solutions (P5726) were purchased from Sigma-Aldrich (St. Louis, MO). Mouse CD34 antibody (MA1-22646, Thermo Scientific, Rockford, IL), mouse CD34-Alexa 488 antibody (553373, R&D Systems, Minneapolis, MN), mouse CD31-PE antibody (553373, BD Pharmingen, San Diego, CA), VEGFR2 antibody (MAB5718, 1:4000, R&D Systems, Minneapolis, MN), Gapdh antibody, Alexa 488-conjugated secondary antibody to mouse (A11001, 1:200, Invitrogen), and horseradish peroxidase (HRP)-conjugated secondary antibody to rabbit (HAF008, 1:2000, R&D Systems, Minneapolis, MN) were purchased and stored following the manufacturer's guidelines.

Preparation of LMWH-DOCA conjugates. DOCA derivatives were synthesized by the chemical conjugation of deoxycholic acid and lysine or lysine substituents containing 2-4 amine groups using a building block method (1). They are referred to as the monomeric, dimeric, trimeric, and tetrameric deoxycholic acids (*mono*DOCA, *bis*DOCA, *tri*DOCA, *tetra*DOCA, respectively). Prior to conjugating with LMWH, DOCA derivatives were further reacted with ethylenediamine (EDA) to introduce a focal primary amine at each DOCA derivative. LMWH-DOCA conjugates were synthesized by chemical coupling of hydrophilic LMWH backbone with amine conjugated DOCA derivatives (*mono*DOCA-NH_2, *bis*DOCA-NH_2, *tri*DOCA-NH_2, and *tetra*DOCA-NH_2).

LMWH (100 mg) was dissolved in 3.125 mL FA at an accelerated temperature. DOCA derivatives were also dissolved in a co-solvent system of DMF/FA. The carboxylic groups of LMWH were activated using EDAC/NHS and reacted with DOCA derivatives at different feed model ratios ranging from 1:12 at 4ºC for 12 h. The reacted materials were then precipitated in an excess of cold ethanol followed by drying in vacuum after centrifugation. The dried heparin conjugates were dissolved in water prior to lyophilize. The synthesis of LMWH-DOCA conjugates was confirmed using ^{1}H NMR, which showed specific amide bonds and bile acid peaks in the specific ppm range. Relative anticoagulant activity of the LMWH-DOCA conjugates was determined by a kinetic method using an anti-factor Xa (anti-FXa) chromagenic assay kit and a chromagenic substrate (S2222) sensitive to FXa according to the principle of the assay (2). The conjugation ratio was determined as described by Fini *et al* with some modifications (3).

Binding affinity studies. Affinity measurements of LMWH and its conjugates with commercially available human full-length prion protein (PrP; ab140567, Abcam) and doppel (ab139778, Abcam) protein were performed by surface plasmon resonance on a BIAcore T100 (GE Healthcare). Both proteins retained more than 90% purity (PrP >90% and doppel >95%) according to the manufacturer. Proteins reconstituted in RNAse free water and stored at -80ºC as described by the manufacturer. Detailed information on these recombinant proteins can be found on manufacturer website. Using standard EDAC-NHS coupling method, recombinant proteins were immobilized at a density of 4000-7000 onto a sensor chip (GE Healthcare). Measurements were performed at a flow rate of 20 µL/min, and 50 mM NaOH was used to regenerate the chip surface after each cycle of analysis. Each concentration was analyzed in duplicate. Kinetic

analysis of the data obtained was performed using BIAcore T100 evaluation software (GE Healthcare).

Pharmacokinetics and Bio-distribution studies. For pharmacokinetic experiments, Sprague Dawley (SD) rats (male, weighed 250-260 g) were randomly divided into two groups (n = 4-5 for each group) for LMWH and LHbisD4 . Treated samples, at a dose of 10 mg/kg, were administered orally mixing with labrasol and Poloxamar 188 (BASF Aktiengesellschaft, Germany). Blood was collected at 15 min, 30 min, 1, 2, 3, 4, 6, and 8 h after drug administration. Plasma was isolated by centrifugation at 4,000xg for 20 min. The amount of drugs in the plasma was measured by heparin-orange chemosensor kit. Heparin orange chemosensor kit (Heparin Orange G26; MW 675.57), obtained from Professor Yang-tae Chung from Lumino Genomics Laboratory of National University of Singapore, was used to detect the plasma concentrations of the samples as previously described in the literature (4). In brief, heparin orange, a chemo sensor material that reacts with heparin conjugates, has a reaction pattern that is mostly charge-charge interactions and the resulting complex emits luminescence.

Biodistribution of LHbisD4 in tumor tissues was performed in a separate group of SCC7-tumor-bearing mice (n = 3-4 for each time point) by a method described previously (5). For all biodistribution studies we used a fluorescent marker for tracking LHbisD4. Mice were administered LHbisD4–Cy5.5 by oral gavage (10 mg/kg). Mice were perfused with PBS buffer (30 mL) at pre-designated time points (0.5, 2, 4, 8 and 24 h). The fluorescent Cy5.5 was extracted from the tissues by incubation with formamide for 48 h at 25ºC. Samples were centrifuged and signal intensity of fluorescence of supernatants was detected with a Wallac 1420 VICTOR plate-reader (Perkin-Elmer Life Sciences) with excitation/emission at 670 nm/720 nm.

The results were normalized to protein levels in the corresponding tissues. Tissue autofluoresence was corrected by subtracting the fluorescent signal of non-treated tumors from the respective readings in treated mice. The amount of LHbisD4 was calculated as per gram of tissue. Similarly, levels of fluorescent signal in mouse sera were measured at different time points (15 min, 30 min, 1, 2, 3, 4, 6, 8, 10 and 24 h) using excitation/emission readings at 670 nm/720 nm.

Tumor Models. SCC7 ($1x10^6$ cells) cells were subcutaneously inoculated at the dorsal flank of C3H/HeN mice (male, 6-7 weeks old, n = 6-8, Orient Bio Inc., Seongnam, Korea). When tumors reached 50-70 mm^3, mice were treated orally with LHbisD4 (10 mg/kg) daily for three weeks. Mice were sacrificed when tumors reached a volume greater than 2.5 cm^3. MDA-MB-231 cells were injected into Balb/c nude mice (female, 6-7 weeks old, n = 6-8, Orient Bio Inc., Seongnam, Korea). LHbisD4 (2.5, 5, and 10 mg/kg) was administered every day by oral gavage. For another group of mice, LHbisD4 was administered twice daily at doses of 5 and 10 mg/kg. Mice were sacrificed when tumors reached a volume greater than 1.8 cm^3.

Immunohistochemistry. Paraffin sections were deparaffinized, incubated with proteinase K, heated at 95°C for 20 min in citrate buffer (pH 6.0) (Invitrogen), and treated with peroxidase blocking reagent (Dako). Sections were incubated with antibody against anti-human CD34, anti-mouse CD31, and PCNA followed by an HRP-conjugated secondary antibody (Dako) and visualized by DAB (diaminobenzidine) staining. Sections were lightly counterstained with hematoxylin.

Immunofluorescence staining of clinical samples. Paraffin-blocked tissue sections or tissue microarrays (TMA) were incubated in a 60ºC dry oven for melting the paraffin. Melted paraffin sections were deparaffinized and rehydrated by using a series of alcohol-xyline (2x10 min, RT) with vigorous shaking, ethanol (99%; 5 min, RT), ethanol (90%; 5 min, RT), ethanol (80%; 5 min, RT), ethanol (70%; 5 min, RT), and PBS (at least 1 min, RT). For antigen retrieval, tissue sections were immersed in a 0.01M citrate buffer bath and placed into a steamer. After operating for 1 hour, the slides were cooled to room temperature for 30 min. Slides were washed vigorously in a PBS bath for 2 times and immersed in hydrogen peroxide solution for 15 min. After washing with PBS (2 times), sections were incubated with 100-200 µL of blocking solution (1x) in a humidified chamber for 1 h at RT. After blocking, tissue sections were incubated with primary antibody for overnight at 4ºC. Antibody solution was prepared in blocking buffer. For the detection of doppel from human testis, 100 µL of diluted antibodies were used as follows- rabbit anti-doppel (HPA043373, 1:100, Human Protein Atlas), goat (G-20) anti-doppel (sc-16863, 1:40, Santa Cruz), goat (N-20) anti-doppel (sc-16862, 1:40, Santa Cruz), and rabbit (FL-20) anti-doppel (sc-25657, 1:40, Santa Cruz). For the detection of doppel from clinical cancer and normal tissues, 100 µL of diluted antibodies were used as follows- rabbit anti-doppel (1:40) and goat anti-doppel (G-20; 1:40). For the detection of doppel from TMA, 200 µL of goat anti-doppel (G-20; 1:40) antibody was used. All of the TMA and clinical cancer tissues were co-stained with mouse anti-human CD34 antibody (QBend10, 1:50, Biocare Medical, CA). For each experiment, one slide was served as a negative control and incubated with control IgG instead of the primary antibody. After overnight incubation, antibody solutions were removed from the samples by tapping the slides on a paper and inserting the slides into a beaker with TBST. Slides were washed three times for 5 min with gentle agitation. In the meantime, secondary antibodies

were prepared in 5% BSA containing Hoechst dye (1:1000). For doppel and CD34 detection, sections were simultaneously stained with 100-200 μL of Alexa 488-linked donkey anti-mouse (1:200; Invitrogen) and Alexa 546-linked donkey anti-goat (1:200; Invitrogen) secondary antibodies for 2 h at RT. Slides were washed as stated before. Excess TBST was removed from the samples by tapping the slides on a paper and covering them with mounting medium, using a cover glass on each slide. The slides were checked under a confocal microscope (Carl Zeiss LSM710, Leica DM IRB/E; Leica Co., Germany).

Whole mount and immunofluorescence staining of mouse tumor tissues. Paraffin embedded mouse tissue sections were pretreated as mentioned before. For whole mount staining, tumors were dissected and cut into pieces (plug) of approximately 2 mm x 2 mm using a scalpel. The plugs were fixed in methanol containing 25% DMSO for 24 h at 4ºC in a 50 mL reaction tube. The plugs were washed three times (at least 30 min each time) with sterile PBS at 4ºC with gentle agitation. The plugs were blocked for 3 h with 5% BSA at 4ºC under gentle agitation. The tumor plugs were incubated in blocking buffer containing the primary antibody overnight at 4ºC under gentle agitation. In another group, tumor plugs were incubated with control IgG instead of the primary antibodies. Next day, the plugs were washed three times with TBST for 3 h at 4ºC under gentle agitation. The plugs were incubated in blocking buffer (5% BSA in TBST) containing the fluorescence-labeled secondary antibody overnight at 4ºC under gentle agitation. After washing for 3 h at 4ºC under gentle agitation the plugs were stained with hoechst dye. Finally, the plugs were embedded in mounting medium and sealed the slides with pertex so that they cannot dry out. The three dimensional structure of the capillary network was analyzed by confocal microscopy. For doppel and CD31 detection, plugs or tissue sections were

simultaneously stained with goat anti-doppel (G-20; 1:40), followed by Alexa 488-linked donkey anti-goat and PE-linked rat anti-mouse CD31 antibodies. For the control IgG, plugs were incubated with goat IgG, followed by Alexa 488-linked donkey anti-goat and PE-linked rat anti-mouse CD31 antibodies. For CD137 and CD31 detection, sections were simultaneously stained with rat anti-mouse CD137, followed by Alexa488-linked goat anti-rat and PE-linked rat anti-mouse CD31.

Conditioned media (CM). When cancer cells reached confluence in 100 mm dishes, the normal growth media were replaced with 10 ml serum free media. After 24 h incubation, the supernatant was centrifuged and filtered through 0.2 mm syringe filters (Corning). The resulting CM were stored in aliquots at -80 °C.

Sorting of tumoral endothelial cell (TEC). Tumoral endothelial cells were isolated using double marker and followed by a procedure published earlier with some modifications. Briefly, tumors were grown subcutaneously in the flank of C_3H/HeN mice and resected, minced using two surgical blades, and digested in 9 mL collagenase and 1 mL dispase solution per gram of tissue. Tissues were incubated for 30 min in a 37ºC water bath, under continuous agitation. Subsequently, 75 uL DNaseI solution per 10 mL cell suspension was added and incubated for another 30 min at 37ºC with continuous agitation. Digested tissues were sieved through a 100-µm cell strainer and single cells were separated. Cells were collected by centrifugation at 400xg for 7 min at room temperature. To remove red blood cells, granulocytes, nonvital cells and cell debris, cells were resuspended in 10 mL Ficoll separation medium (per gram of starting material) and carefully layer the suspension on 7.5 mL Ficoll-Paque (pre-warmed to room temperature).

The interphase-containing viable cells were transferred into a fresh tube. Cells were collected into FACS tubes, and incubated with anti-mouse CD31-PE and anti-mouse CD34-FITC antibodies (at a final concentration of 2 μg/mL). FACS machine was prepared by adjusting conditions with a sheath fluid pressure of 29.9 psi, a sorting frequency of 44 kHz and a plate voltage of 3,500 V. Collected cells were suspended in 10 mL ECGM containing 10% FBS and centrifuged. Then finally, cells were plated in 0.2% gelatin coated 100 mm dishes and cultured overnight in TEC growth media that is supplemented ECGM containing 10% FBS and 10% CM. Next day, the media was replaced with fresh TEC growth media. Cells were grown for 2-3 days until confluent. For different experiments, all the TECs were used between passage no. (P) 1 to 5 with population doublings up to 15.

Doppel cDNA transfections in human umbilical endothelial cells. To overexpress doppel in HUVECs or luciferase expressing HUVECs (Hu^{+luc}), cells were transfected with lipofectamine 2000® following manufacturer's instructions. Briefly, cells (5x105 cells, P#1) were grown in culture media (ECGM) in 100 mm dishes. Cells were grown for 5 days. The culture media was changed every other day. Cells (P#2) were subcultured in 60 mm dishes ($0.7x10^5$ cells per dish) for doppel cDNA transfection. At day 1 of subculture, cells were transfected accordingly. On the day of transfection, doppel cDNA was re-suspended in 100 uL of RNAse-free water, and the following reagents were prepared. Solution A: for each transfection, 0.5 ug of doppel cDNA and mock cDNA was diluted with 145 μL OptiMEM (51985; Gibco) in different tubes. Solution B: for each transfection, 5 μL of lipofectamine 2000® was diluted with 145 μL of OptiMEM. The reaction mixtures were incubated for 5 min at RT. The cDNA solution (Solution A) was directly added to the diluted transfection reagent (Solution B). The solution was mixed gently by

pipetting up and down and the mixture was incubated for 20 min at RT. Before transfection, the cells were washed once with 2 mL of OptiMEM media. For each transfection, 0.7 mL OptiMEM media was added to each well and allowed to prime for a few minutes. The transfection reagent mixture (Solution A + Solution B) was added and gently mixed. For lipofectamine 2000® only, 0.85 mL of OptiMEM was added to well and diluted transfection reagent (Solution B) was mixed gently. Thirty minutes after transfection, 1.0 mL of normal growth media was added and toxicity was not observed. When growth culture media was added 1~4 h after transfection, moderate to severe toxicity was observed. The transfection was allowed for 24 h before the cells were subjected to subsequent experiments. For generating stable cell lines, the cells were isolated using FACS after labeling with goat (G-20) anti-doppel antibody. Additionally, sorted cells (P#3) were grown in culture media containing 1000 μg/mL of selective agent (G418 sulfate; PAA Laboratories GmbH, Austria) for 7 days without further expansion. Only viable cells retained expression plasmids, which were stably integrated into the cell genome. The expression of doppel was evaluated from the whole cell lysates of doppel transfected HUVECs and non-transfected HUVEC. The stability of doppel expression was monitored *in vitro* for more than 30 days. Doppel transduced Hu^{+luc} were used *in vivo* in passages between 3-5 with the maximum population doublings of 15-20.

Knockdown of doppel in Hu.dpl cells. Briefly, Hu.dpl cells ($5x10^5$ cells, P#3~4) were grown in culture media in 100 mm dishes. Cells were grown for 5 days by changing the culture media every other day. Cells were then sub-cultured in 60 mm dishes ($0.7x10^5$ cells per dish) and grown for 2 days until they became 60~70% confluent. At day 2 of subculture, cells were divided into three groups and transfected accordingly. For Solution A, 1.0 μg of human doppel

esiRNA (EHU154061; Sigma-Aldrich) and scramble siRNA were diluted with 95 µL OptiMEM. For Solution B, 5 µL of Mission® siRNA transfection reagent (S1452; Sigma-Aldrich) was diluted with 95 µL of OptiMEM. Solution A and B were mixed and incubated for 30 min at RT. The mixture was added and gently mixed over cells. One day later, the transfection efficiency was checked using western blot analysis.

Doppel knockdown in tumor endothelial cells. TECs, isolated from SCC7 tumor, were grown in (35x10 mm) gelatin coated 6 well dishes for 21-24 h with supplemented ECGM with antibiotics. 60-80% confluent cells were used for transfection. On the day of transfection, Doppel shRNA was resuspended in 200 uL of RNAse-free water. For each transfection, 15 µL of shRNA duplex (sc-42205-SH; stock: 0.1 ug/uL; Santa Cruz) was diluted into 85 µL shRNA plasmid transfection medium and 10 µL of shRNA Transfection Reagent was diluted into 90 µL shRNA plasmid transfection medium. The shRNA duplex solution was added directly to the diluted transfection reagent using a pipette. The mixture was gently pipetted and incubated for 30-40 minutes at room temperature. Cells were washed once with 2 mL of shRNA Plasmid Transfection Medium. For each transfection, 0.8 mL shRNA plasmid transfection mixture was overlay onto the washed cells. The cells were incubated for 4 h at 37°C in a CO_2 incubator. 4 h later, 1 mL of normal growth medium containing 2 times the normal serum and antibiotics concentration (2x normal growth medium) was added without removing the transfection mixture. The cells were additionally incubated for 24 to 72 h. The knock down efficiency was confirmed by checking the doppel expression. The doppel knock down TEC is termed as $TEC^{-/-dpl}$. For the generation of stable cell line, doppel expression was knock down by transducing shRNA using lentiviral particles (sc-42205-V; Santa Cruz) following a method published previously (6). Briefly, TECs

at passage 1 were seeded, allowed to adhere, and grown in complete media. On the day of transfection, the cells should be 50~60% confluent. Polybrene (sc-134220, Santa Cruz) solution was prepared in complete media at a concentration of 5 μg/mL and added. TECs were then infected overnight with doppel shRNA lentiviral particles or control shRNA lentiviral particles (sc-108080, Santa Cruz) at a final multiplicity of infection of 10. Next day, the transfection media was replaced with culture media (without polybrene) and grown overnight. Knockdown efficiency was monitored by FACS analysis. For generating stable cell lines, doppel shRNA transfected cells were incubated with Dynabeads (110.35 [mouse], Invitrogen) that were pre-coated with goat (G-20) anti-doppel antibody (5 μL per 50 μL of bead suspension). Magnet was applied for separation of Dynabeads and bead-captured cells. These are positively isolated cells that express doppel. The un-captured cells were transferred to a new tube. These are the negatively isolated cells that represent knockdown cells. These steps were repeated for three times to ensure the isolation of purified and viable $TEC^{-/-dpl}$ cells. Negatively isolated cells were directly monitored using FACS to confirm the isolation efficiency. Isolated $TEC^{-/-dpl}$ were further expanded for puromycin (sc-108071, Santa Cruz) selection and cultured for 5~7 days. Resulting puromycin-resistant clones were selected as stably transfected cells. For *in vitro* and *in vivo* uses, the population doublings of $TEC^{-/-dpl}$ cells were kept within 10-15.

Quantitative PCR. mRNA was purified using the Quick Prep Micro mRNA purification kit (Amersham, Piscataway, NJ). Single-stranded cDNA was generated using the Superscript III first strand synthesis system (Invitrogen) following the manufacturer's directions. Quantitative PCR was performed with an MX4000 using Brilliant SYBR Green QPCR Master Mix, and threshold cycle numbers were obtained using MX4000 software v. 4.20 (Stratagene, La Jolla,

CA). Conditions for amplification were: one cycle of 95^0C, 10 min followed by 40 cycles of 95^0C, 20 s; 56^0C, 30 s; and 72^0C, 30 s. Quantitative PCRs were performed in triplicate, and threshold cycle numbers were averaged. Gene expression as normalized to that of the 70 Kd U1 small nuclear ribonucleoprotein polypeptide A (*Snrnp70*), a gene that is uniformly expressed in all ECs as assessed by SAGE. Relative expression was calculated using the equation $2^{(Rt-Et)}/2^{(Rn-En)}$ where Rt is the threshold cycle number observed in the experimental sample for Snrnp70, Et is the threshold cycle number observed in the experimental sample for the gene of interest (GOI), Rn is the average threshold cycle number observed for Srnp70 in normal mouse brain endothelium (B.End.3) samples, and En is the average threshold cycle number observed for the GOI in B.End.3 samples. Primers used were-

mouse doppel:

forward: GGACATCGACTTTGGAGCAGAG;

reverse: CAGCATCTCCTTGGTCACGTTG,

mouse Snrnp70:

forward: GCCTTCAAGACTCTGTTCGTGG;

reverse: CTCGATGAAGGCATAACCACGG,

Generation of EC spheroid and subcutaneous implantation in mice. The spheroid based *in vivo* angiogenesis assay was performed according to the procedure published earlier (7). Briefly, TECs were isolated from SCC7 tumor, cultured, and transfected using lentiviral vector to knock down doppel, as described in supplementary methods. $8x10^6$ TECs or $TEC^{-/-dpl}$ were suspended in 200 mL media containing 20% methocel solution and 80% culture medium. Cells were divided into non-adherent plastic square petri dishes into 25 μL for each spheroid. Spheroids

formed by TECs or $TEC^{-/-dpl}$ were harvested and mixed in a matrigel/fibrin mixture that contained mouse VEGF and bFGF. TECs or $TEC^{-/-dpl}$ Spheroids (1000 spheroids per plug) were inoculated subcutaneously in the flank of each female SCID mice (5-6 weeks, Jungang Animal Lab, Korea) or female Balb/c nude mice (Orinet bio, Seongnam, Korea). The spheroids were allowed to grow for 3 weeks. Cy5.5 labeled LMWH was injected intravenously at the dose of 2.5 mg/kg, and at 2 h after injection, its accumulation at the site of TEC implantation was checked using Optimax-MX3 (GE Medical Systems, Milwaukee, WI). In other experiments, Cy5.5 labeled LHbisD4 was administered orally at the dose 10 mg/kg, and its distribution was also checked as described previously. Finally, the matrix plug was removed and part of the plugs was analyzed for microvessel density, drug accumulation by immunofluorescence staining, and to measure the hemoglobin content by Drabkins reagent.

To check the relation between doppel expression and angiogenesis, either luciferase expressing HUVEC (Hu^{+luc}) or doppel-transfected HUVEC ($Hu^{+luc+Dpl}$) spheroids were generated and similarly grafted in the flank of SCID mice as mentioned earlier. The spheroids were allowed to grow for 3 weeks. The growing human vasculature was monitored using bioluminescence imaging. Images were captured at every 3 min intervals using IVIS Xenogen-200 imaging system after intraperitoneal D-luciferin injection. Finally, the maxtrix plug was removed and part of the plugs was analyzed for human microvessel density (antibody against human CD34) by whole mount, immunohistochemistry, and immunofluorescence staining.

In-vivo near-infrared fluorescence imaging and tumor localization studies. For tumor imaging, LHbisD4–Cy5.5 (10 mg/kg) was administrated orally into the SCC7-tumor-bearing mice (n = 3). Time-course fluorescent images were captured on IVIS Xenogen-200 imaging system. Excised

tumor and organs were also imaged after treating mice from separate studies (n = 2 mice at each time points). Fluorescence intensities of *ex vivo* tumors were quantified and normalized to the value of the liver. Different tumor models were also used to demonstrate the universal application of LHbisD4 in tumor localization. LHbisD4–Cy5.5 (10 mg/kg) was administrated orally to MDAMB-231, A549, HT29, HCT119, CT26, HepG2 and HN9 tumor-bearing mice (n = 1 for each tumor model). Then, the mice were monitored at pre-designated time points. For the microscopic analysis of the tumor vasculatures, whole mount or tissue sections from the LHbisD4–Cy5.5 treated tumors were prepared and analyzed by confocal microscopy after labeling with either doppel antibody or CD31 antibody.

Phospho-RTK signaling array, immunoprecipitation, pull-down, and immunoblotting assays. Cells were analyzed by the PathScan RTK Signaling Ab Array (Cell Signaling) Kit following the manufacturer's directions. Immunoblot analysis was performed essentially as described (8). Briefly, equal amounts of protein were resolved by SDS-PAGE and blotted onto nitrocellulose membranes (GE Healthcare). After blocking, membranes were probed with an anti-doppel antibody, anti-pVEGFR2 antibody, anti-VEGFR2 antibody, anti-pAKT antibody, anti-Erk1/2 antibody, anti-Src antibody, anti-GAPDH antibody, and anti-actin antibody. Different gel concentrations varying from 7.5–13.5% was used for immunoblotting according to the protein's molecular weight. For immunoprecipitation, 0.8–1 mg lysates were incubated with VEGFR2 antibodies (rabbit-x-VEGFR2 for human endothelial cells and goat-x-VEGFR2 for TECs) or doppel antibodies (goat (N-20)-x-doppel for human endothelial cells and rabbit (FL-176)-x-doppel for TECs) as per experimental design. Immunocomplexes were captured with protein G-

Agarose beads (Invitrogen). Beads were washed with IP buffer at least three times, heated in SDS buffer at 100ºC for 5 min, and subjected to SDS-PAGE analysis.

Deglycosylation experiments. TEC lysates were treated with 1000 U of PNGase F and/or 100 U of neuraminidase (Sigma Aldrich) according to a protocol described previously (9). Chemical deglycosylation by trifluoromethanesulfonic acid (TFMS) was also performed following a method published earlier with modifications (10). Briefly, 1 mg of TEC lysate was treated with TFMS for 3 h at 37ºC. The proteins were precipitated and lyophilized. The precipitated proteins were collected by centrifugation, resuspended in SDS sample buffer, and subjected to SDS-PAGE analysis in 13.5% gel.

Proximity ligation assay. For PLA, at first cells were grown, fixed in 4% PFA for 20 min, and thereafter subjected to *in situ* PLA using a Duolink Detection kit (Olink Bioscience, Uppsala, Sweden) following the manufacturer's instructions. Briefly, slides were blocked, incubated with goat (G-20) anti-doppel and rabbit (FL-176) anti-doppel antibodies for detecting doppel protein, goat anti-VEGFR2 (AF644; R&D Systems) and rabbit anti-VEGFR2 (55B11; Cell Signaling) antibodies for detecting VEGFR2 protein, and rabbit (FL-176) anti-doppel and goat anti-VEGFR2 antibodies for detecting VEGFR2/Doppel interaction, and thereafter incubated with PLA probes, which are secondary antibodies (anti-rabbit and anti-mouse, respectively) conjugated to unique oligonucleotides. Ligation of the oligonucleotides was followed by an amplification step. The products were detected by using a complementary fluorescently labeled probe. Cells were further stained with either FITC labeled phalloidin for membrane staining. Slides were mounted using mounting media and evaluated using the confocal microscope.

VEGFR2 internalization assay. To analyze cell-surface retention of VEGFR2, TECs were incubated with or without rabbit (FL-176) anti-doppel antibody, goat anti-VEGFR2 Ab (R&D Systems), and LHbisD4 at a concentration of 10 μg/mL and stained with rabbit anti-VEGFR2 Ab (Cell Signaling) by a method described previously (11). Cells were analyzed in a FACS II flow cytometer (BD Biosciences). For internalization experiments, TECs were exposed to VEGF, rabbit (FL-176) anti-doppel antibody (10 μg/mL), and rabbit IgG. Cells were then washed, fixed, permeabilized, and incubated with anti-VEGFR2 Ab (Cell Signaling), anti-EEA1 Ab (Abcam), and anti-LAMP1 (Abcam) Ab as described. Cells were analyzed on a confocal laser microscope.

TEC sprouting experiment. TEC spheroids were prepared as described in the literature (12, 13). In brief, TECs were grown in gelatin coating dishes, trypsinized, and suspended in endothelial cell growth media (ECGM) and methocel (4:1). Methocel was prepared by dissolving 6 g of methylcellulose (Sigma–Aldrich, Korea) in 500 mL of ECGM. The mixture was centrifuged and the clear supernatant was used as methocel. TEC spheroids were prepared by a hanging drop method such that 1000 ECs in a hanging drop (25 μL) were cultured overnight at 37°C under 5% CO_2 and 100% humidity. The generated spheroids were harvested and suspended in the methocel solution containing 20% FCS (Cambrex, Verviers, Belgium). Subsequently, the ice-cold collagen solution (rat tail type I in 0.1% acidic acid) was mixed with 10% MEM 199 (10X, GIBCO; Invitrogen, CA), followed by adding 10% 0.2 N NaOH to adjust the pH to 7.4. TEC spheroids were mixed at 1:1 ratio in the methocel solution with the neutralized collagen solution, mixed with mouse VEGF (50 ng/mL, Peprotech, Germany) and 0.9 mL of the mixed solution containing 50 TEC spheroids were pipetted into individual wells of a 24-well plate to be

polymerized for 30 min at 37°C under 5% CO_2 and 100% humidity. For the inhibition studies, rabbit (FL-176) anti-doppel antibody and LHbisD4 at different concentration were also mixed with the collagen solution. VEGF activates TECs, thereby inducing the formation of tube-like TEC structures (sprouting TEC). The plates were incubated at 37°C under 5% CO_2 and 100% humidity for 24 h. Sprouting TEC spheroids were photographed and quantitatively determined by counting the cumulative sprout branch points per spheroid using light microscope (Nikkon Ltd., Japan).

Statistical analysis. Nonparametric and normally distributed data were analyzed by unpaired one-tailed Mann-Whitney *U* test and 2-tailed Student's *t* test, respectively, using GraphPad Prism version 6.0c. Kruskal-Wallis nonparametric ANOVA followed by Dunn's *post-hoc* tests were used for multiple comparisons. *P*-values less than 0.05 were considered to be statistically significant. Results are presented as mean ± SEM.

Supplemental Tables

Supplemental Table 1. Characterization of LHbisD4 in comparison to its generic compound LMWH and their dye conjugates.

	Prion Proteins	K_D[a] (nM)	Anti-FXa[b] activity (IU/mg)	Papp[c] x 10^{-7} (cm/sec)
LMWH	PrP	119	100 ± 0.0	6.8 ± 0.6
	Doppel	436		
LMWH-Cy5.5	PrP	108	- - -	- - -
	Doppel	513		
LHbisD4	PrP	248	0.0 ± 0.0	60.1 ± 6.0*
	Doppel	7.8		
LHbisD4-Cy5.5	PrP	302	- - -	- - -
	Doppel	8.8		

[a] The dissociation rate constants (K_D) of LMWH and LHbisD4 with recombinant cellular prion protein (PrP) and prion-like protein (Doppel), measured using surface plasmon resonance

[b] Relative anticoagulant activity

[c] Apparent permeability; polarized transport of LMWH and LHbisD4 in Caco-2 cells at 37°C for 1 h. * $p < 0.001$ vs LMWH.

Supplemental Table 2. Pharmacokinetic (PK) parameters of LMWH and LHbisD4 in rats

	C_{max} (μg/mL)	T_{max} (h)	AUC (μg*h/mL)	$t_{1/2}$ (h)	Cl (mL/h/kg)	Vd (L/kg)	MRT (h)	BA (%)
Intravenous administration								
LMWH (1 mg/kg)	- - -	- - -	8.4 ± 0.7	1.3 ± 0.2	0.09 ± 0.01	0.18 ± 0.02	- - -	- - -
LHbisD4 (5 mg/kg)	- - -	- - -	79.6 ± 15.7	2.0 ± 0.3	0.05 ± 0.0	0.14 ± 0.02	- - -	- - -
Oral administration								
LMWH (10 mg/kg)	0.7 ± 0.0	0.5 ± 0.0	2.5 ± 1.6	- -	- - -	- - -	4.4 ± 0.4	3.0 ± 0.3
LHbisD4 (10 mg/kg)	9.3 ± 1.4	3.0 ± 0.0	36.8 ± 7.2	- -	- - -	- - -	3.2 ± 0.6	23.4* ± 4.6

Results are the means ± standard error mean

C_{max}; Maximum effective concentration

T_{max}; Time to reach maximum effective concentration

AUC; Area under the concentration-time curve from 0 to 8 h

Cl; Clearance

Vd; Volume of distribution

MRT; Mean residence time

BA; Absolute bioavailability

* $p < 0.001$ vs LMWH

Supplemental Figures

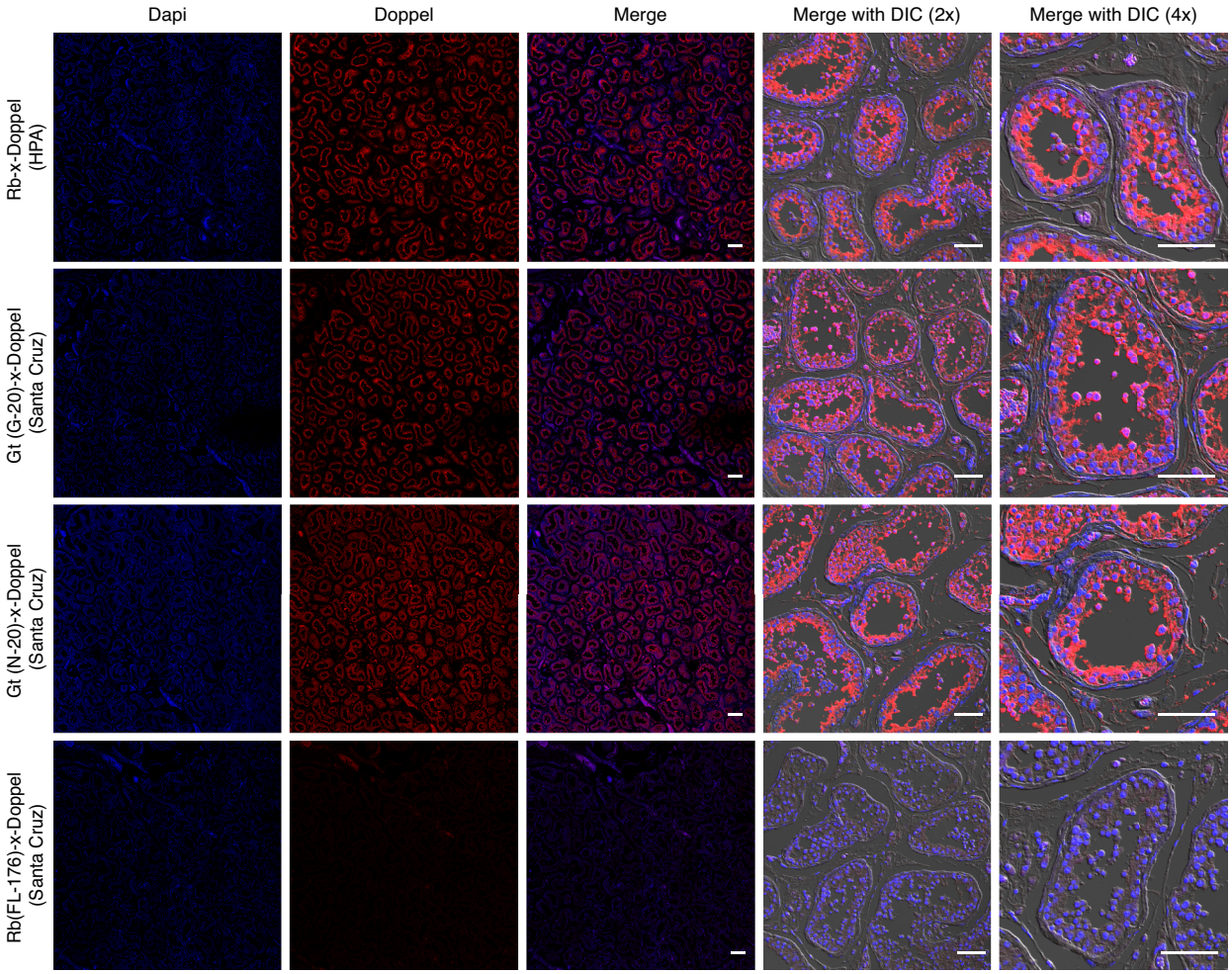

Supplemental Figure 1. Characterization of doppel antibodies in human testis. Among the different antibodies applied, the rabbit anti-doppel from Human Protein Atlas (HPA), the goat (G-20) and the goat (N-20) anti-doppel antibodies from Santa Cruz showed specificity for human doppel in testis tissues by immunofluorescence staining, but the rabbit (FL-176) anti-doppel antibody did not show specificity. Scale bars: 50 μm, 20 μm, and 10 μm.

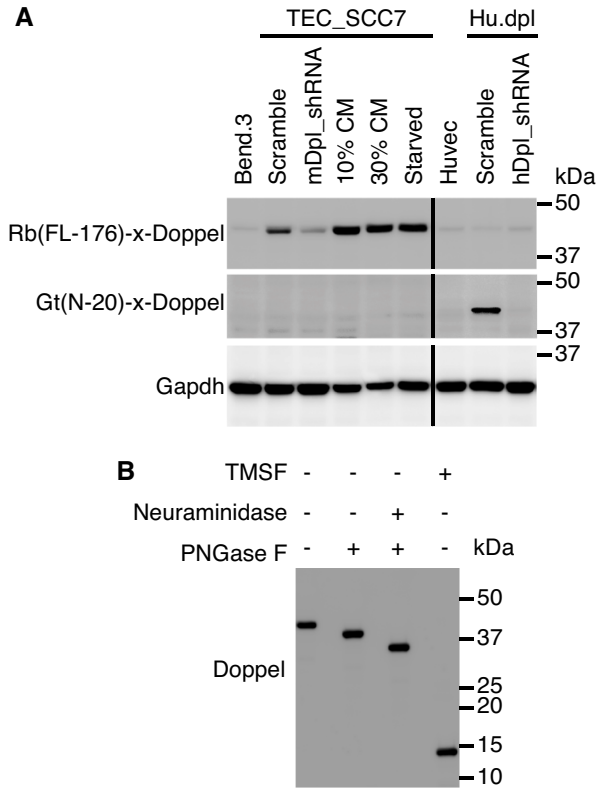

Supplemental Figure 2. Specificity of doppel antibodies in cells. (**A**) Strong doppel signals were observed in the lysates of tumor endothelial cells derived from SCC7 tumor (TEC_SCC7), but not in the normal endothelial cells derived from mouse brain (Bend.3) or human umbilical cord (Huvec), by rabbit (FL-176) anti-doppel antibody. It is noteworthy that the signal of doppel in TECs was highly reduced when cells were treated with shRNA specific to mouse doppel, which confirms the specificity of the antibody. On the other hand, the goat (N-20) anti-doppel antibody showed specificity to human doppel protein only when transfected to Huvec (Hu.dpl). The specificity of antibody was also confirmed by the absence of a strong signal in doppel knockdown Hu.dpl. The expression of doppel in TECs was stable when grown in the presence or absence of conditioned media (CM). See also Supplemental Figure 6B. (**B**) Enzymatic deglycosylation of doppel protein by PNGase F and neuraminidase and chemical deglycosylation by trifluoromethanesulfonic acid (TFMS) in TEC lysates.

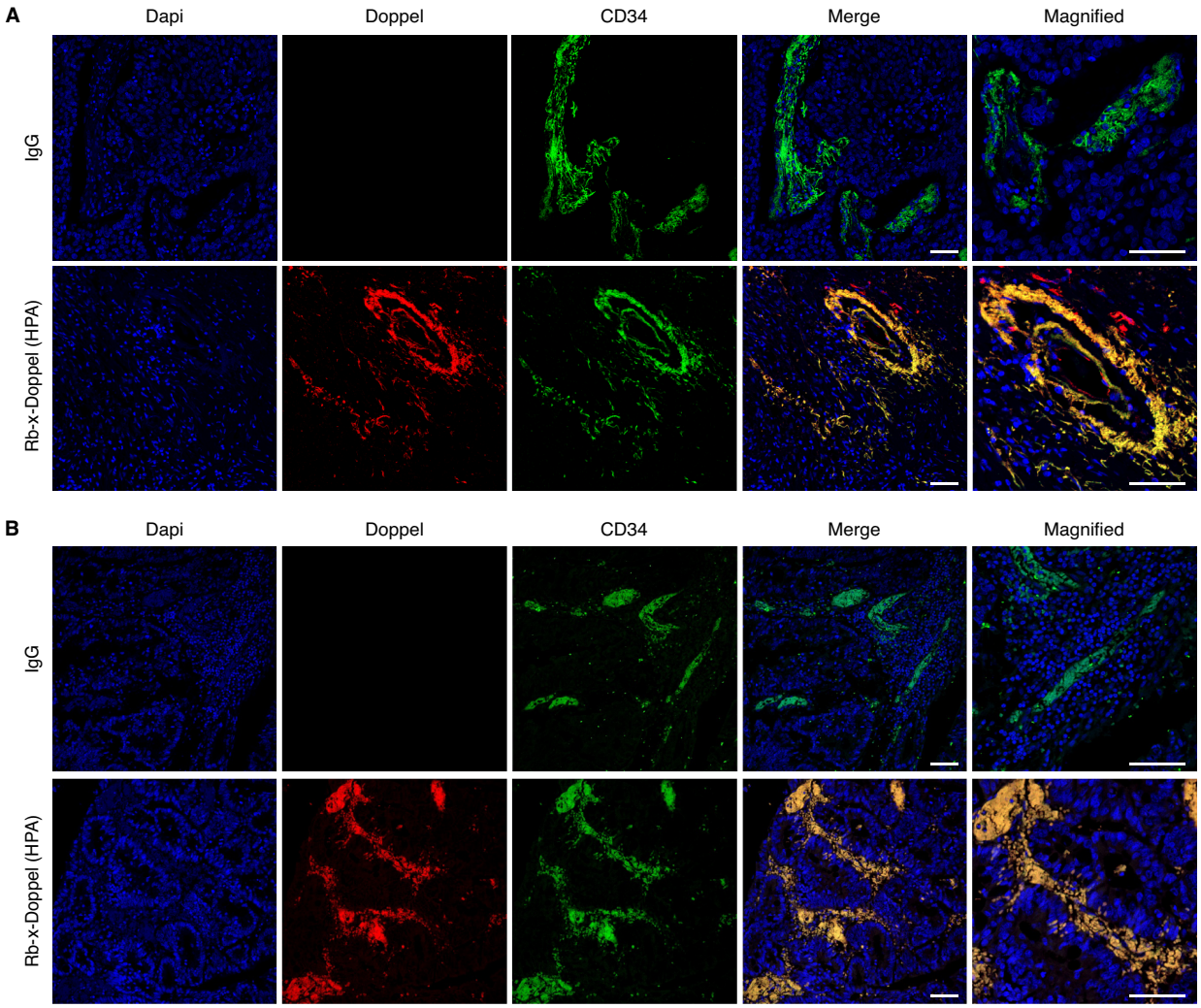

Supplemental Figure 3. Detection of doppel by rabbit anti-doppel antibody from Human Protein Atlas (HPA) in clinical lung and colon cancer tissues. Images showing doppel and blood vessels (CD34) were co-localized in lung (**A**) and colon (**B**) cancer tissues; however, control rabbit IgG failed to detect the expression of doppel in cancer tissues, confirming the specificity of the antibody and immunofluorescence detection method. Scale bars: 20 μm and 10 μm.

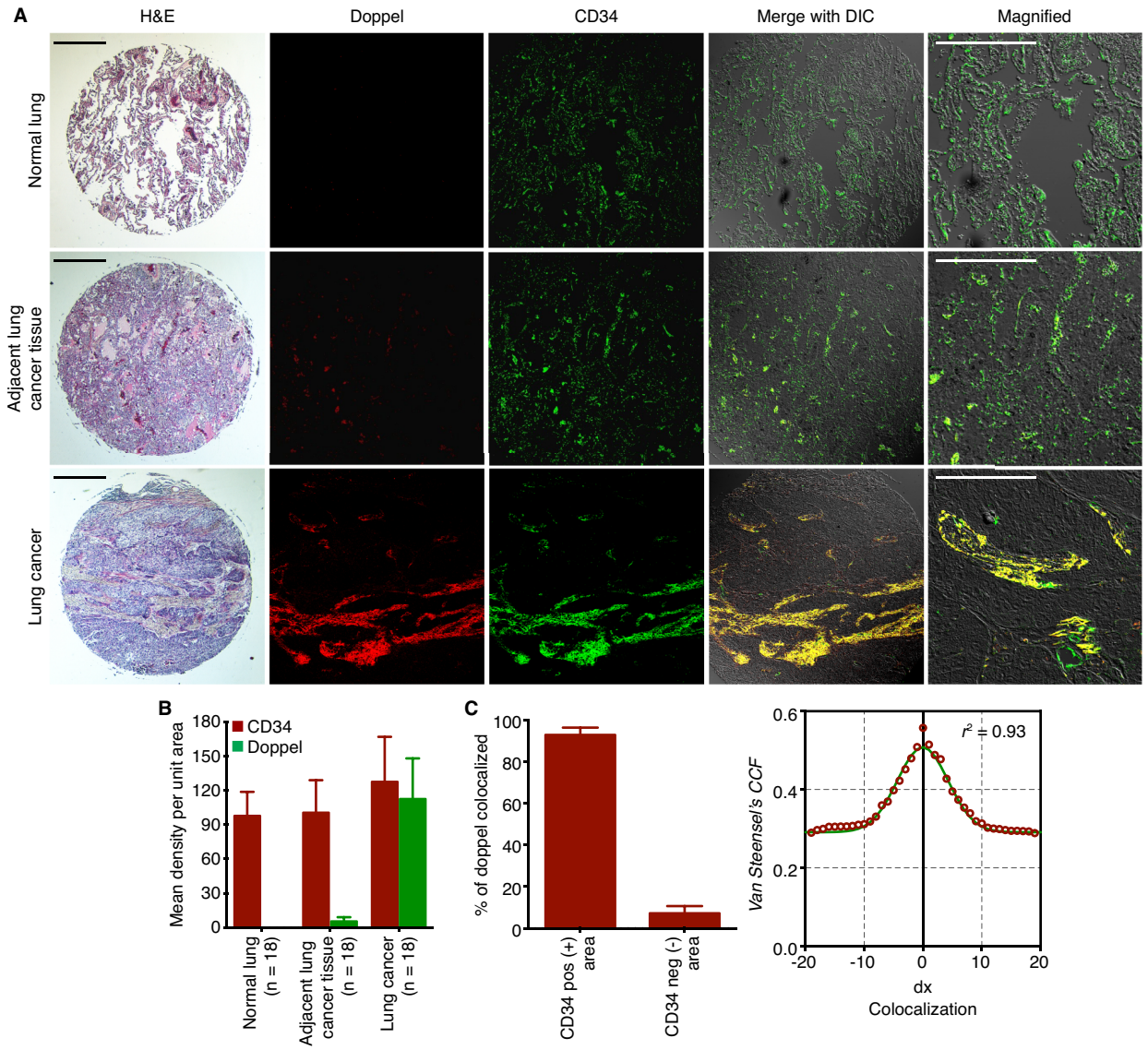

Supplemental Figure 4. Expression of doppel in the human lung cancer tissue microarrays (TMA). (**A**) Representative images of lung cancer TMA stained for doppel (red), blood vessels (green), and nuclei (blue). Scale bar: 50 µm and 20 µm at magnifications. Sections treated with hematoxylin and eosin for morphological references are also shown. Scale bar: 100 µm. DIC means differential interference contrast. (**B**) Quantification of hCD34-positive and doppel-positive blood vessels density. (**C**) Doppel expression was strongly associated with $CD34^+$ positive areas in normal, adjacent, and cancer tissues from lung TMA (left panel). The co-localization analysis was performed on original images using Van Steensel's cross-correlation

coefficient (CCF) between doppel and CD34 using JACop software and Pearson coefficients (*r*) ranging from 0.8 to 1; a bell-shaped curve was observed (right panel).

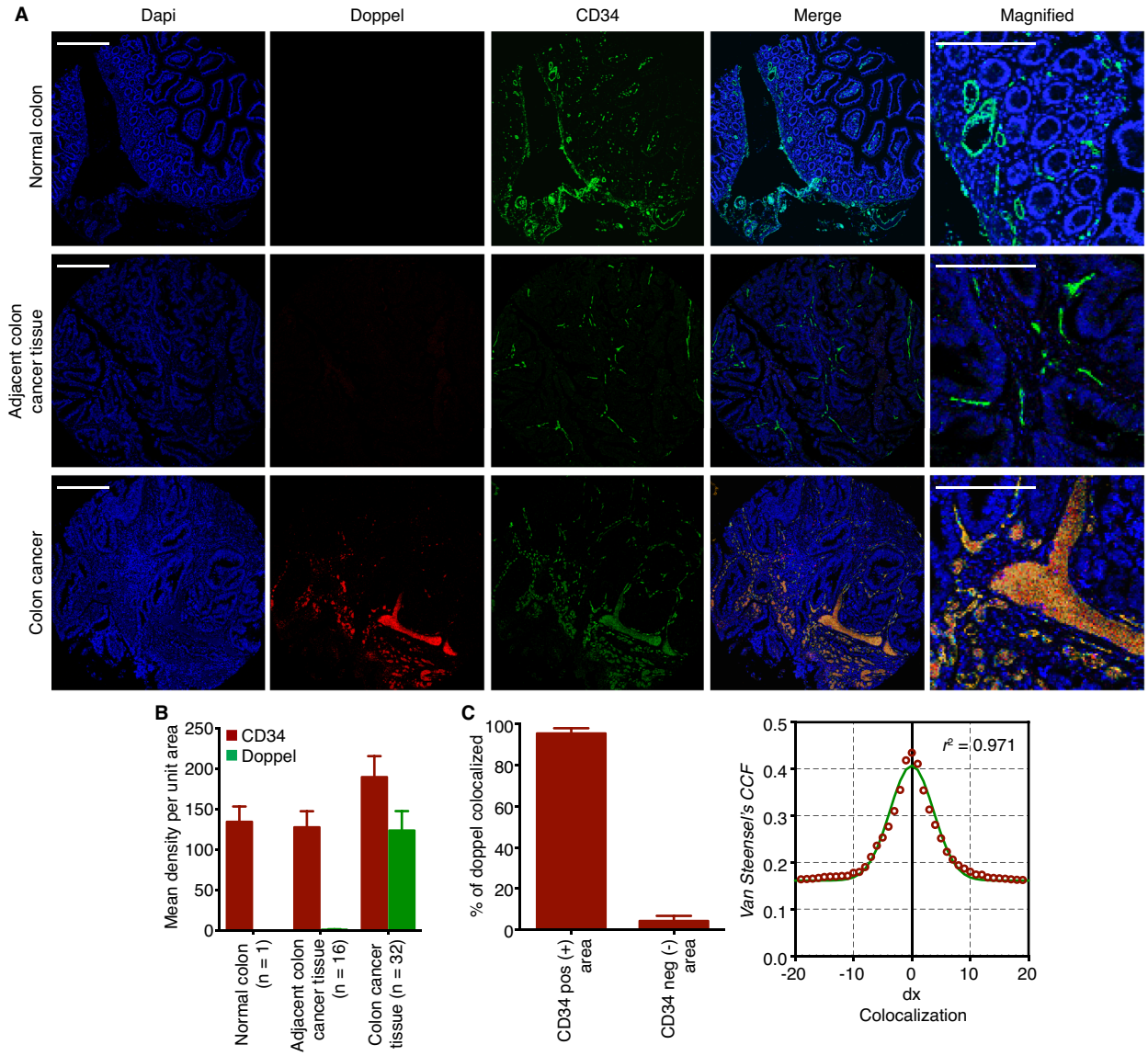

Supplemental Figure 5. Doppel expression in human colon cancer tissue microarrays (TMA). (**A**) Representative images of colon cancer TMA stained for doppel (red), blood vessels (green), and nuclei (blue). (**B**) Quantification of hCD34-positive and doppel-positive blood vessels density in the images. Scale bar: 50 µm and 20 µm at magnifications. (**C**) Doppel expression was strongly associated with $CD34^{+}$ positive areas in normal, adjacent, and cancer tissues from colon TMA (left panel). The co-localization analysis was performed on original images using Van Steensel's cross-correlation coefficient (CCF) between doppel and CD34

using JACop software and Pearson coefficients (*r*) grater than 0.9; a bell-shaped curve was observed (right panel).

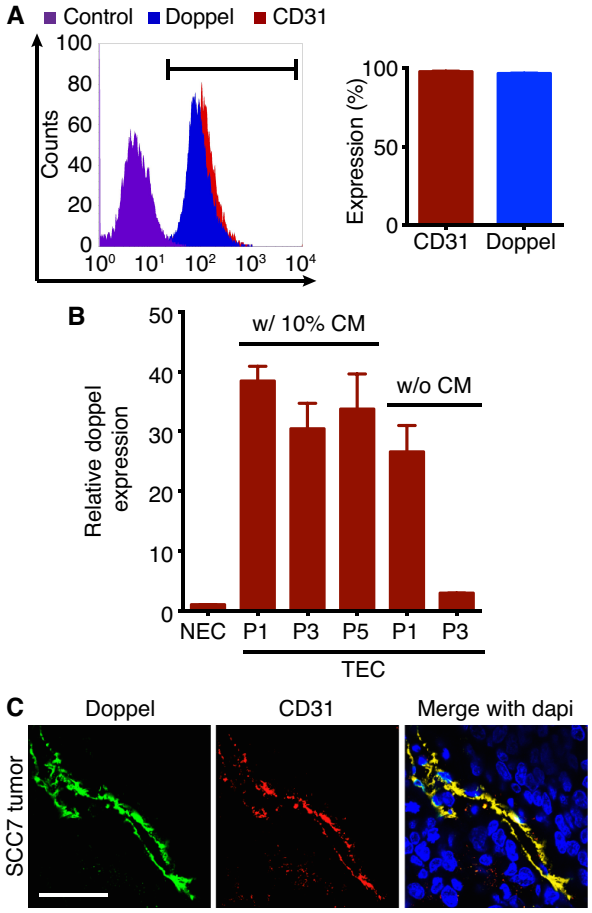

Supplemental Figure 6. Isolation of tumor endothelial cells (TEC), their in vitro stability in culture conditions, and expression in tumor tissues. (**A**) The expression of doppel in isolated TECs derived from SCC7 tumor. (**B**) The expression of doppel in TEC from passage to passage, P1 to P5, when grown in the presence or absence of 10% conditioned media (CM). (C) Immunofluorescence staining for doppel (green), CD31-positive blood vessels (red), and nuclei (blue) in a mouse xenograft SCC7 tumor. Scale bar: 10 μm.

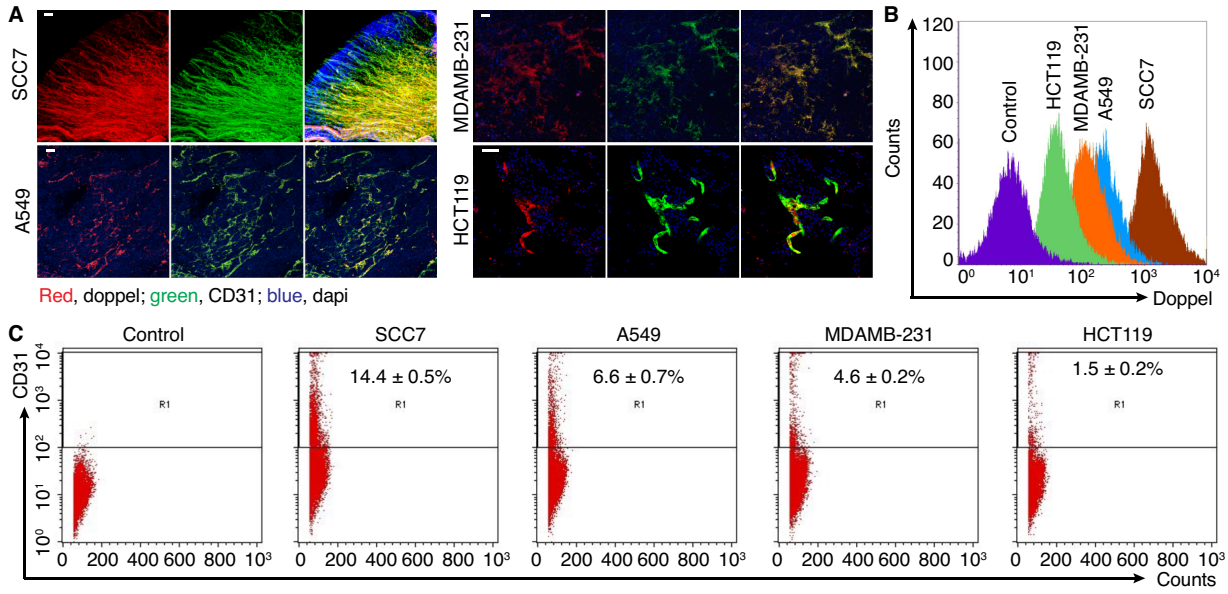

Supplemental Figure 7. Doppel expression is correlated with tumor angiogenesis. (**A**) Doppel is highly expressed in the blood vessels of subcutaneously implanted squamous (SCC7), lung (A549), breast (MDA-MB-231), and colon (HCT119) tumors. Scale bars: 50 μm and 20 μm for HCT119. (**B**) Doppel expression in individual TECs isolated from four different tumors, as determined by FACS analysis. n = 3 experiments. (**C**) FACS analysis of total volume of blood vessels in squamous, lung, breast, and colon tumors. n = 3 sections from each tumor.

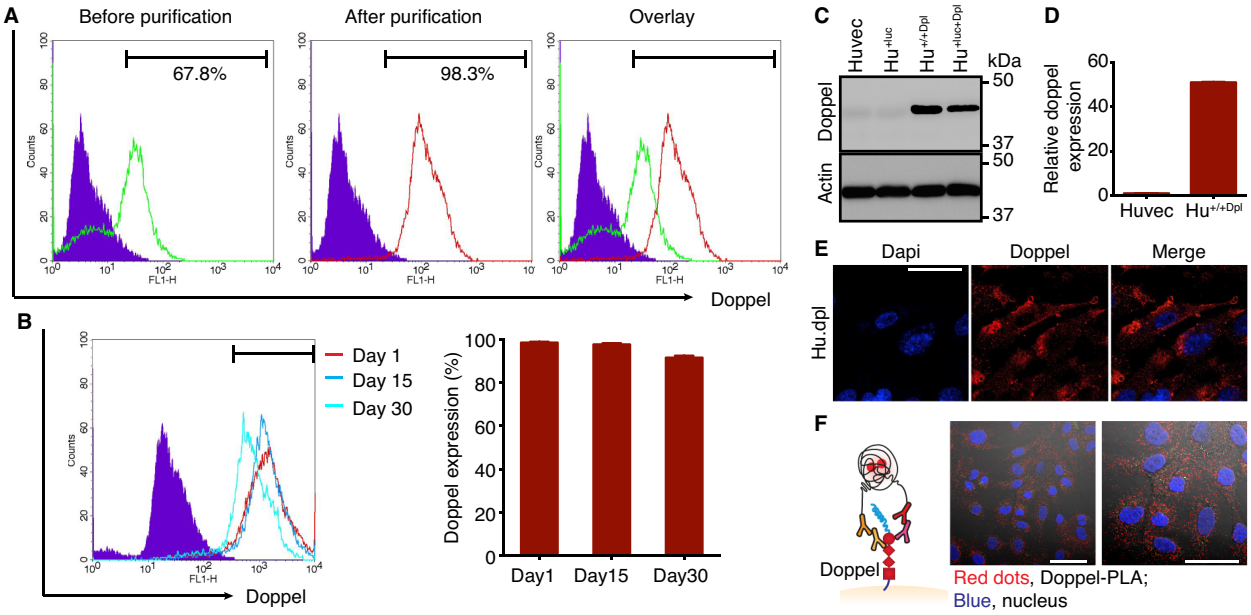

Supplemental Figure 8. Characterization of doppel transfection in luciferase expressing Huvec (Hu^{+luc}) cells. (**A**) FACS analysis of doppel expression in Hu^{+luc} cells 1 day after its cDNA transfection. Reanalysis of sorted cells shows more than 98% purity. (**B**) *In-vitro* stability of doppel expression in stably transfected Hu^{+luc} cells ($Hu^{+luc+dpl}$) was shown up to 30 days in culture. (**C**) Immunoblotting of doppel in Hu^{+luc} and $Hu^{+luc+dpl}$ cell lysates. (**D**) Relative mRNA expression of doppel in Hu^{+luc} and $Hu^{+luc+dpl}$ cells. (**E**) Immunofluorescence staining of doppel in $Hu^{+luc+dpl}$ cells. Scale bar: 10 µm. (**F**) Representative images of the proximity ligation assay of doppel protein (red dots) in $Hu^{+luc+dpl}$ cells. Nuclei are stained with dapi (blue). Scale bar: 20 and 10 µm. All the experiments were duplicates.

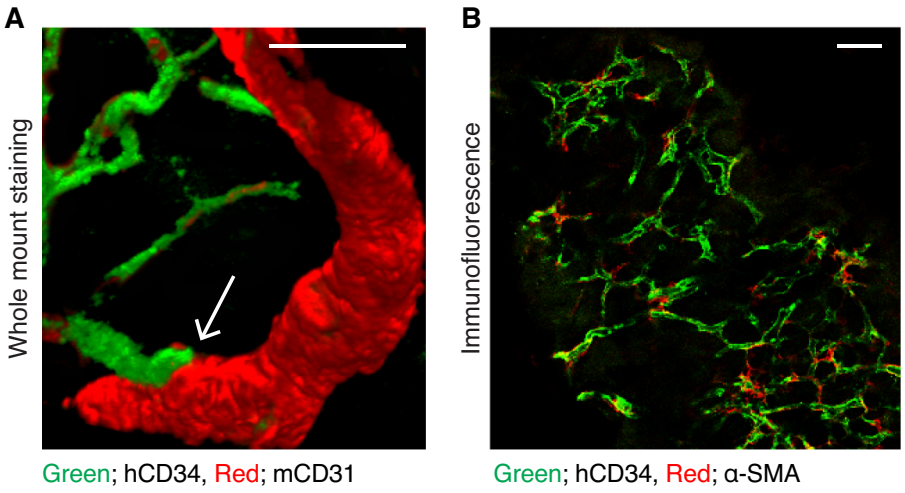

Supplemental Figure 9. Characteristics of human vasculatures formed by transplanted EC spheroids *in vivo*. Pre-characterization and validation of the perfused human vasculature network formation *in vivo* 21 days after the implantation of luciferase transfected HUVEC (Hu^{+luc}). (**A**) Images of whole mount staining for human CD34 (hCD34; green) and mouse CD31 (mCD31; red) showing that human vasculatures are anastomosed with host vasculatures within the plug (n = 3 mice). Arrow indicates the anastomoses between hCD34 and mCD34. Scale bar: 5 μm. (**B**) Immunofluorescence staining of human CD34 (green) and mouse α-smooth muscle actin (α-SMA; red) showing that the outgrowing vessels were partially covered by host mural cells (n = 3 mice). Scale bar: 20 μm.

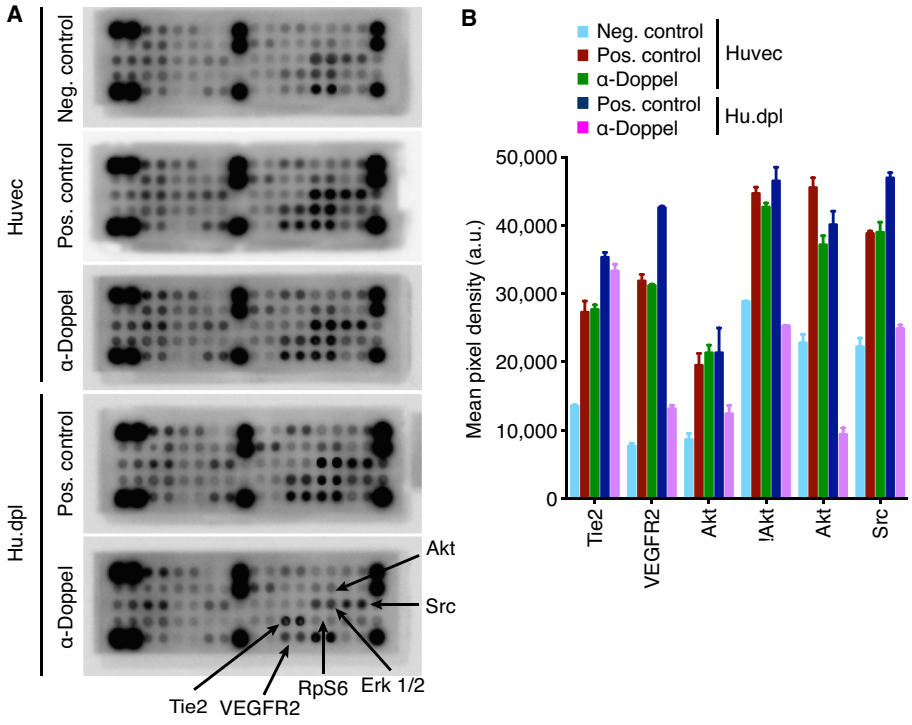

Supplemental Figure 10. **Changes in the phosphorylation pattern of receptor tyrosine kinases (RTK) and their canonical signals due to blocking doppel in endothelial cells.** (**A**) Attenuation of phospho-RTK signaling in HUVECs non-transfected or transfected with doppel (Hu.dpl) when exposed to its blocking antibody (α-Doppel; 30 min, 10 μg/ml) in the presence of complete growth media. (**B**) Quantification of pixel density of phosphorylated Tie2, VEGFR2, Akt, Erk1/2, RpS6, and Src. All the experiments were duplicates.

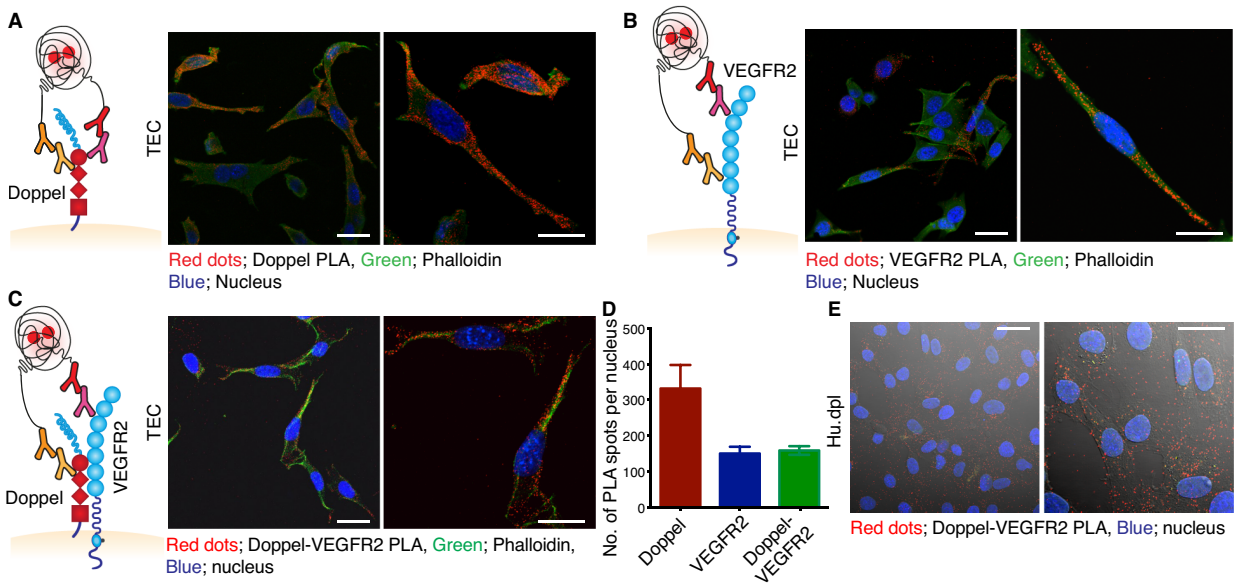

Supplemental Figure 11. Doppel associates with VEGFR2. Representative images of the proximity ligation assay (PLA) of doppel (**A**), VEGFR2 (**B**), and doppel-VEGFR2 interactions (**C**) identifies on TECs. PLA signals are shown in red dots, cytoskeletal staining (FITC-phalloidin) in green, and nuclear staining (dapi) in blue. Scale bars: 20 and 10 µm. (**D**) Quantification of doppel, VEGFR2, and doppel-VEGFR2 heterodimer PLA signals in TECs. (**E**) Representative images of the proximity ligation assay (PLA) of doppel-VEGFR2 interactions identifies on Hu.dpl cells. Nuclei (dapi) are in blue. Scale bars: 20 and 10 µm. All the experiments were triplicate.

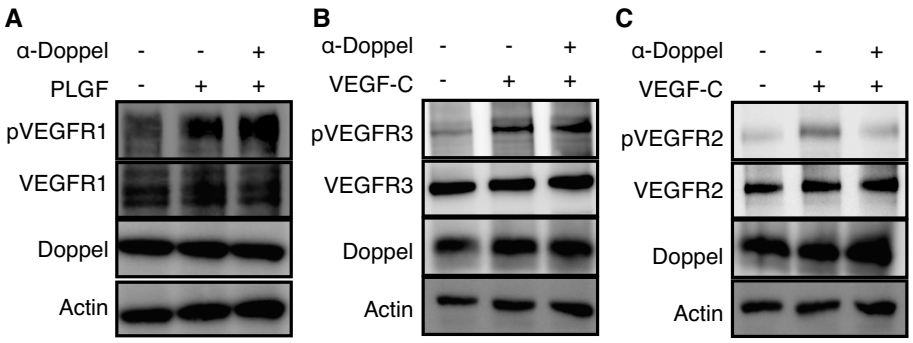

Supplemental Figure 12. Doppel does not attenuate phosphorylation of VEGFR1 and VEGFR3. (**A**) Immunoblot of phosphorylated VEGFR1, total VEGFR1, total doppel, and actin in Hu.dpl when stimulated with PlGF in the presence or absence of α-Doppel. (**B**) Immunoblot of phosphorylated VEGFR3, total VEGFR3, total doppel, and actin in Hu.dpl cells when stimulated with VEGF-C in the presence or absence of α-Doppel. (**C**) Immunoblot of phosphorylated VEGFR2, total VEGFR2, total doppel, and actin in Hu.dpl cells when stimulated with VEGF-C in the presence or absence of α-Doppel. Note that either PlGF-stimulated VEGFR1 phosphorylation or VEGF-C induced VEGFR3 phosphorylation was not affected; however, doppel blocking could attenuate VEGF-C induced VEGFR2 phosphorylation in the same cells. All the experiments were triplicate.

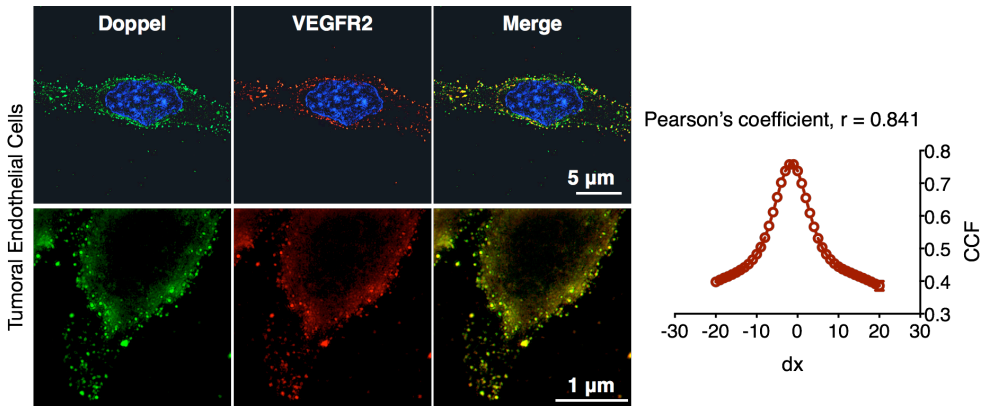

Supplemental Figure 13. Doppel co-localizes with VEGFR2 in surface microdomains and doppel blocking inhibits TEC sprouting. High-resolution confocal microscopy reveals the co-localization of doppel and VEGFR2 on the surface microdomains of TECs. The co-localization analysis performed on original images using Van Steensel's cross-correlation coefficient (CCF) between doppel and VEGFR2 with JACop software. The perfect bell-shaped curves and pearson coefficient (r) ranging from 0.8 to 1 were observed for the doppel and VEGFR2. Scale bars: 5 and 1 µm. All the experiments were triplicate.

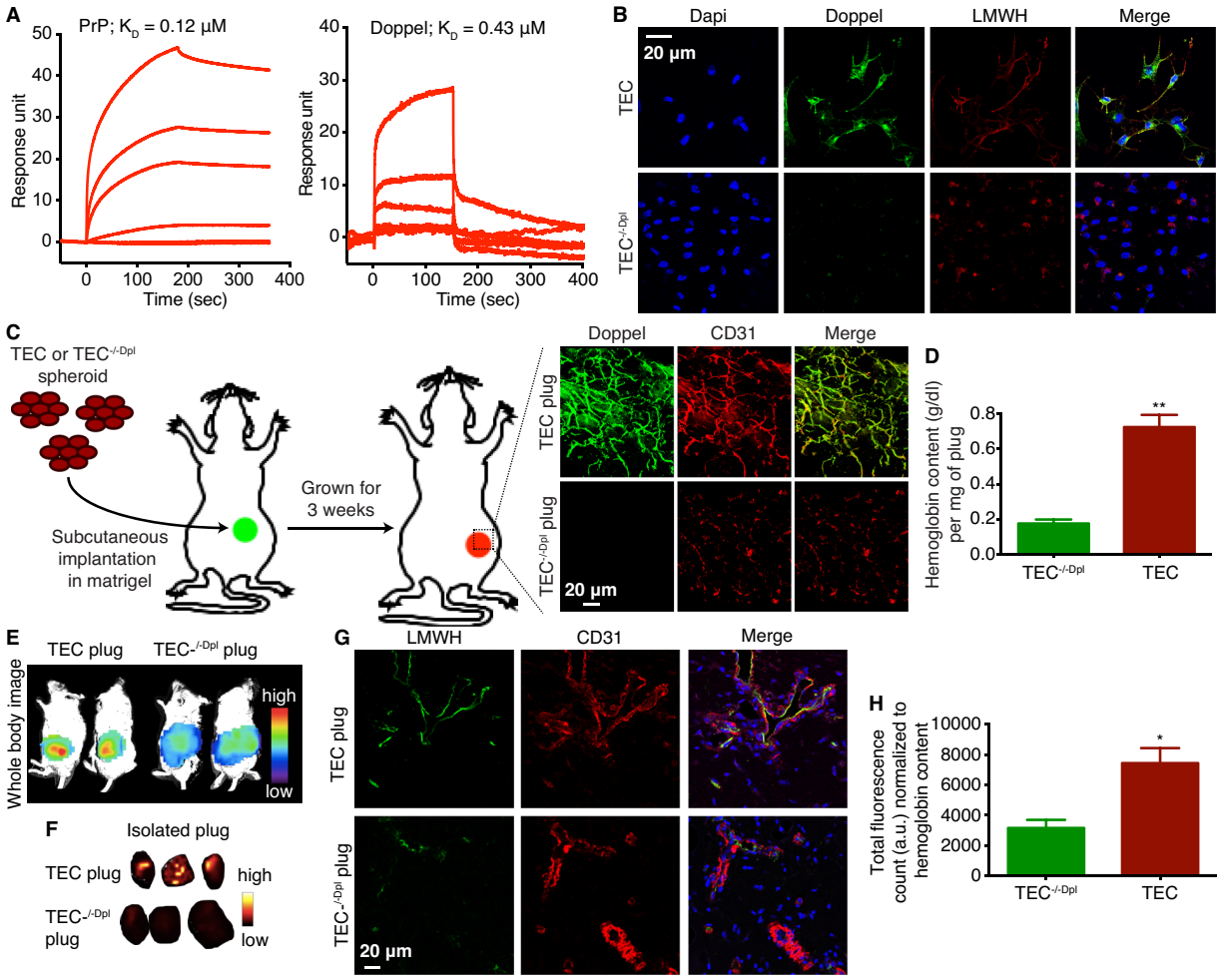

Supplemental Figure 14. Heparin can target doppel on Tumoral endothelial cells (TEC). (**A**) Representative sensograms recorded by surface plasmon resonance of PrP-LMWH and doppel-LMWH (3 experiments). Dissociation rate constants are calculated from the response curves. Sensorgrams representing direct binding kinetics for the indicated compound are shown in response units as a function of time with increasing concentration. (**B**) LMWH binding to TEC and doppel knock down TEC (TEC$^{-/-dpl}$). To be noted, LMWH nonspecifically bound to the surface of TEC$^{-/-dpl}$, but co-localized specifically with doppel on the membrane of TEC. n = 3 experiments (**C**) Schematic diagram of subcutaneously implanted TEC and TEC$^{-/-dpl}$ spheroids in mice that formed perfused vascular network within 21 days of implantation. Doppel staining is shown in green. CD31 (blood vessel marker) staining is shown in red. Scale bar: 20 µm. (**D**)

Hemoglobin contents within TEC and $TEC^{-/-dpl}$ plugs were quantified. *** $p < 0.001$ vs Hu^{+luc}. $n = 3$ plugs. Distribution of Cy5.5 labeled LMWH in subcutaneously implanted TEC and $TEC^{-/-dpl}$ plug, both *in vivo* (**E**) and *ex vivo* (**F**). $n = 3$ mice. (**G**) LMWH localizes to the growing blood vessels of TEC plug, but not the blood vessels of $TEC^{-/-dpl}$ plug. LMWH staining is shown in green. Blood vessel (CD31) staining is shown in red. Nuclei (dapi) staining are shown in blue. Scale bar: 20 μm. $n = 3$ mice. (**H**) Total fluorescence photon count of intravenously injected LMWH in TEC and $TEC^{-/-dpl}$ plug ($n = 3$ plugs). All values were normalized to hemoglobin content of each plug. * $p < 0.05$ for TEC vs $TEC^{-/-dpl}$.

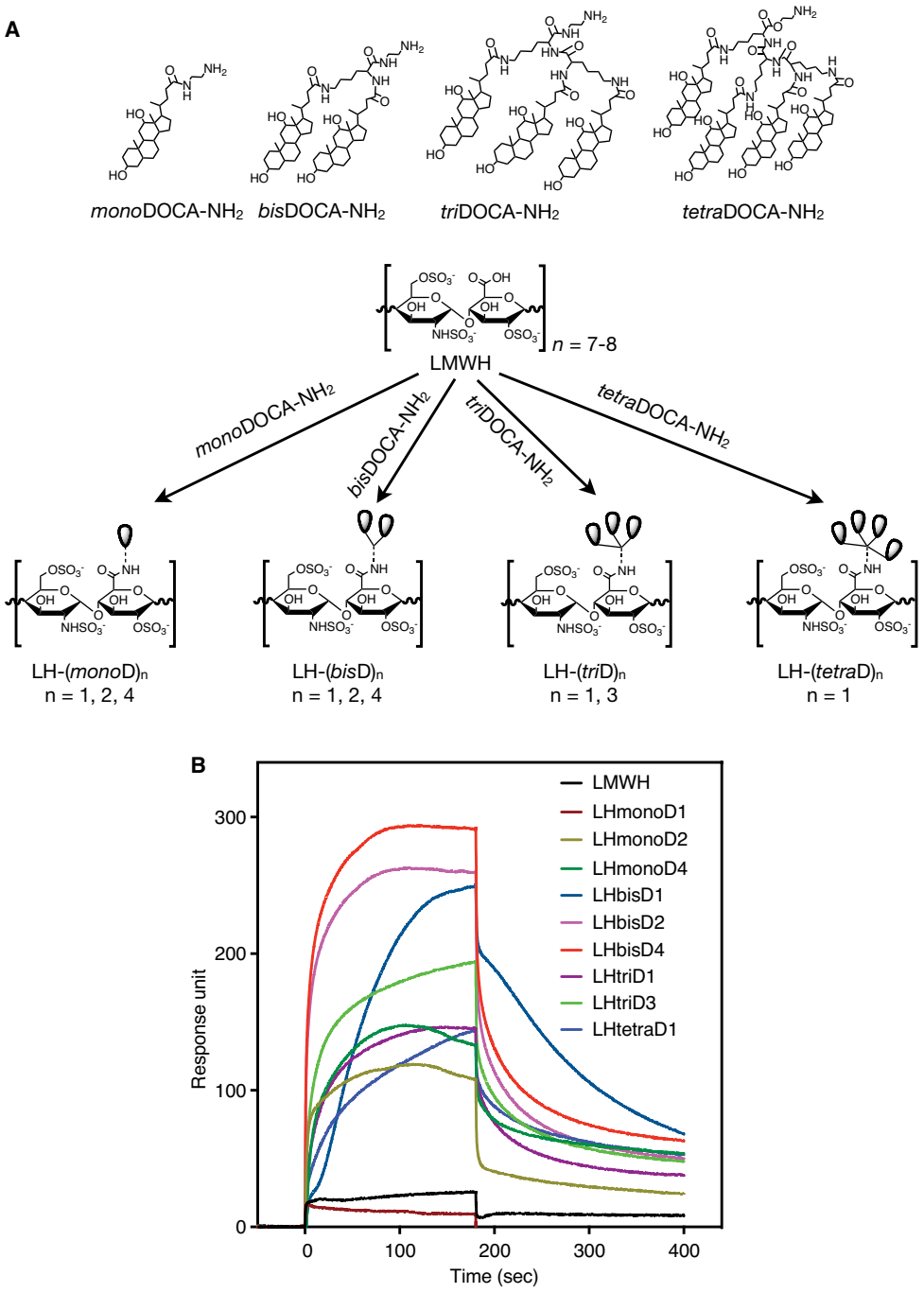

Supplemental Figure 15. Synthesis and screening of heparin-based conjugates for doppel binding. (**A**) The schematic structures of low molecular weight heparin (LMWH) based conjugates that are synthesized to enhance the binding affinity to doppel. Structures showing different oligomer of deoxycholic acid (*oligo*DOCA) derivatives, designated as *mono*DOCA,

*bis*DOCA, *tri*DOCA, and *tetra*DOCA. The structure of LMWH-*oligo*DOCA conjugates that are conjugated with the –COOH groups of saccharide units. Conjugation ratio varies from 1 to 4 molecules per molecule of LMWH. (**B**) Representative sensograms recorded by surface plasmon resonance for doppel and LMWH-*oligo*DOCA conjugates (3 experiments). Sensorgrams representing direct binding kinetics for the indicated compounds are shown in response units as a function of time with a concentration of 1 μM.

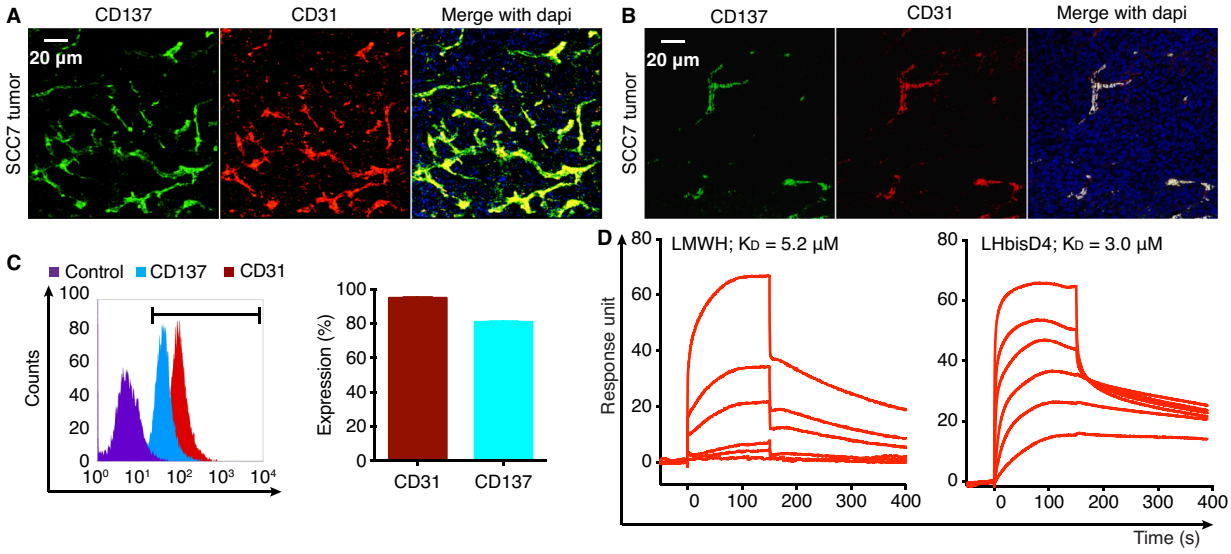

Supplemental Figure 16. LHbisD4 has no increased binding affinity to the known tumor endothelial marker, CD137. (**A**) Whole mount staining of SCC7 tumor section showing CD137 (green) expression in tumor vessels (CD31). Scale bar: 20 μm. (**B**) Immunofluorescence staining for CD137 (green), CD31-positive blood vessels (red), and nuclei (blue) in a mouse xenograft SCC7 tumor. Scale bar: 20 μm. (**C**) The expression of CD137 in isolated TECs derived from SCC7 tumor. (**D**) Surface plasmon resonance analysis between CD137-LMWH (left) and CD137-LHbisD4 (right). Dissociation rate constants are calculated from the response curves. All the experiments were triplicate.

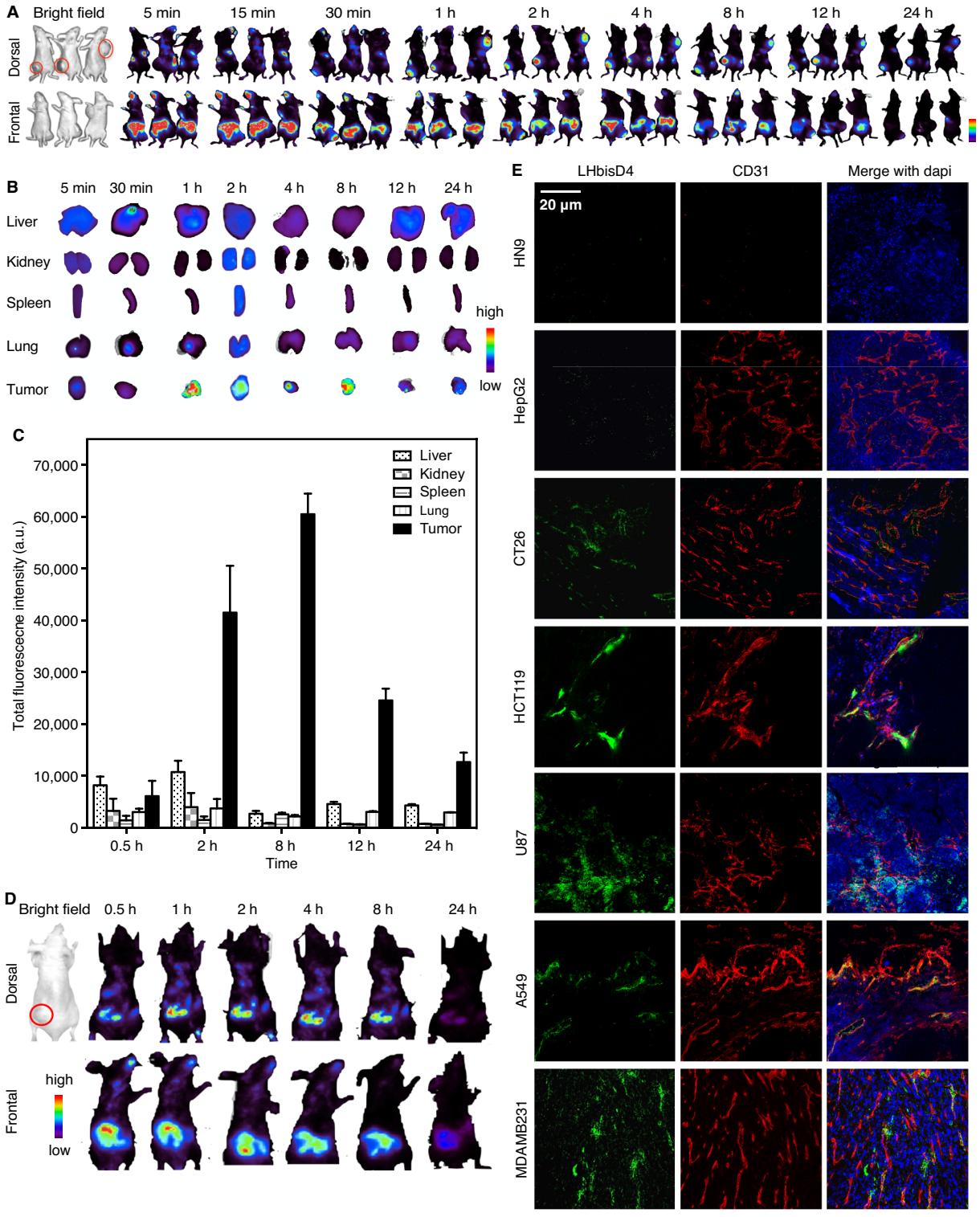

Supplemental Figure 17. Bio-distribution and localization of LHbisD4 in different tumor models. (**A**) Bio-distribution study of Cy5.5 labeled LHbisD4 at different time points in SCC7

tumor bearing mice after its oral administration at a given dose of 10 mg/kg. (**B**) Organ accumulation study of Cy5.5 labeled LHbisD4 at different time points in SCC7 tumor bearing mice after its oral administration at a given dose of 10 mg/kg. (**C**) Total fluorescence intensity of Cy5.5 labeled LHbisD4 in different organs as a function of time when administered orally at a dose of 10 mg/kg (n = 3 at each time points). Results are mean ± s.e.m. To be noted, SCC7 tumor has 23-fold higher accumulation of LHbisD4 over liver after 8 h post oral administration. (**D**) Mice bearing MDAMB-231 breast tumors are orally administered at a dose of 10 mg/kg of Cy5.5 labeled LHbisD4 and NIR fluorescence images at different time points were captured. (**E**) Tumor tissue sections of six different tumor models of different cancer types (head & neck, liver, colorectal, brain, lung, and breast cancers) at 8 h post-administration of Cy5.5 labeled LHbisD4 (n = 3 tumors). LHbisD4 staining is shown in green. Tumor blood vessel (CD31) staining is shown in red. The nuclei (dapi) staining are shown in blue. Scale bar: 20 μm.

Supplemental References

1. Al-Hilal TA, et al. Oligomeric bile acid-mediated oral delivery of low molecular weight heparin. *J Control Release.* 2014;175:17-24.
2. ten Cate H, Lamping RJ, Henny CP, Prins A, and ten Cate JW. Automated amidolytic method for determining heparin, a heparinoid, and a low-Mr heparin fragment, based on their anti-Xa activity. *Clin Chem.* 1984;30(6):860-864.
3. Fini A, Fazio G, Roda A, Bellini AM, Mencini E, and Guarneri M. Basic Choline Derivatives .11. Comparison between Acid and Basic Derivatives. *J Pharm Sci.* 1992;81(7):726-730.
4. Wang SL, and Chang YT. Discovery of heparin chemosensors through diversity oriented fluorescence library approach. *Chem Commun.* 2008;10:1173-1175.
5. Benny O, et al. An orally delivered small-molecule formulation with antiangiogenic and anticancer activity. *Nat Biotechnol.* 2008;26(7):799-807.
6. Compte M, et al. Factory neovessels: engineered human blood vessels secreting therapeutic proteins as a new drug delivery system. *Gene Ther.* 2010;17(6):745-751.
7. Alajati A, et al. Spheroid-based engineering of a human vasculature in mice. *Nat Methods.* 2008;5(5):439-445.
8. Croci DO, et al. Disrupting galectin-1 interactions with N-glycans suppresses hypoxia-driven angiogenesis and tumorigenesis in Kaposi's sarcoma. *J Exp Med.* 2012;209(11):1985-2000.
9. Peoc'h K, et al. The human "prion-like" protein Doppel is expressed in both Sertoli cells and spermatozoa. *J Biol Chem.* 2002;277(45):43071-43078.
10. Edge AS, Faltynek CR, Hof L, Reichert LE, Jr., and Weber P. Deglycosylation of glycoproteins by trifluoromethanesulfonic acid. *Anal Biochem.* 1981;118(1):131-137.
11. Croci DO, et al. Glycosylation-dependent lectin-receptor interactions preserve angiogenesis in anti-VEGF refractory tumors. *Cell.* 2014;156(4):744-758.
12. Korff T, and Augustin HG. Tensional forces in fibrillar extracellular matrices control directional capillary sprouting. *J Cell Sci.* 1999;112 (Pt 19):3249-3258.
13. Laib AM, Bartol A, Alajati A, Korff T, Weber H, and Augustin HG. Spheroid-based human endothelial cell microvessel formation in vivo. *Nat Protoc.* 2009;4(8):1202-1215.